

Electrophysiological Properties of Rat Vestibular Labyrinth and Their Effect on Parameters of Transmitted Voltage Pulses

V. P. Demkin¹, V. V. Udut^{1,2}, P. P. Shchetinin¹, M. V. Svetlik¹,
S. V. Mel'nichuk¹, A. P. Shchetinina¹, M. O. Pleshkov¹,
D. N. Starkov¹, O. V. Demkin¹, and H. Kingma^{1,3}

Translated from *Byulleten' Eksperimental'noi Biologii i Meditsiny*, Vol. 164, No. 12, pp. 671-676, December, 2017
Original article submitted July 13, 2017

We propose a new approach to optimization of electrical stimulation of the vestibular nerve and improving the transfer function of vestibular implant. A mathematical model of the vestibular organ is developed based on its anatomy, the model premises, 3D-analysis of MRI and CT images, and mathematical description of physical processes underlying propagation of alternating electric current across the tissues of vestibular labyrinth. This approach was tested *in vitro* on the rat vestibular apparatus and had been examined anatomically prior to the development of its mathematical model and equivalent electrical circuit. The experimental and theoretical values of changes of the gain—phase characteristics of vestibular tissues in relation to location of the reference electrode obtained in this study can be used to optimize the electrical stimulation of vestibular nerve.

Key Words: *vestibular implant; in vitro vestibular apparatus; anatomic structure; mathematical model; stimulating voltage pulses*

The physical processes underlying the passage of an electric current across the tissues of vestibular labyrinth are vigorously studied in many labs [9,11]. These studies are needed to improve the parameters of vestibular implant (VI) for the patients with bilateral vestibular hypofunction [7,12]. The transfer function of VI depends on the placement configuration of electrodes in tissues the vestibular organ, which strongly affects the gain—phase characteristics of the pathway for electric current employed to stimulate the afferent nerve and seriously limits broad-scale use of modern VI [10]. Special attention should be focused on position of the reference electrode used as a common lead when measuring the gain—phase characteristics of

vestibular tissues, which affects the nerve-stimulating electric current, so the correct selection of this position can optimize the parameters of VI electrical pulses [10].

In view of strict ethic regulations of the experiments with patients, on the one hand, and different properties of cadaveric and vital tissues, on the other hand, the use of laboratory mammal animals seems to be an effective approach to optimization of electrical stimulation of vestibular nerve, because anatomy and physiology of their vestibular apparatuses are similar to those in humans. The pivotal feature in this approach is the development of an *in vitro* electrophysiological model of vestibular organ with precisely positioned stimulating, recording, and reference electrodes, on the one hand, and elaboration of a mathematical model with equivalent electrical circuit based on 3D visualization of high-resolution MRI and CT images, on the other hand, which together can yield reliable gain—phase characteristic of the vestibular tissues needed to describe transformation of stimulating electric pulses from generator to the nerve [1,4,6].

¹National Research Tomsk State University; ²E. D. Goldberg Research Institute of Pharmacology and Regenerative Medicine, Tomsk National Research Medical Center, Russian Academy of Sciences, Tomsk, Russia; ³Department of Otorhinolaryngology and Head and Neck Surgery, Division of Balance Disorders, Faculty of Health Medicine and Life Sciences, Maastricht University Medical Center, School for Mental Health and Neuroscience, Maastricht, the Netherlands.
Address for correspondence: wospp@yandex.ru. P. P. Shchetinin

This work was designed to study the anatomical structure and electrophysiological properties of rat vestibular organ to develop its mathematical model describing propagation of alternating electric current across the vestibular labyrinth to the vestibular nerve.

MATERIALS AND METHODS

Experiments were carried out on outbred male Wistar rats weighing 300-350 g ($n=10$) obtained from Breeding Department of the Tomsk National Research Medical Center. The animals had no visible signs of neuropathology or physical defects. The rats were maintained under standard vivarium conditions with water and food *ad libitum*. All procedures were carried out in strict adherence to European Convention for the Protection of Vertebrate Animals used for Experimental and Other Scientific Purposes (Strasbourg, 1986) and in compliance to the principles of Good Laboratory Practice.

To examine the anatomical structure of vestibular organ, the rats were decapitated under ether narcosis, soft tissues of the periotic region were removed, and the skull was trepanized. The bones of the tympanic cavity and periotic capsule were extracted with preserved native structure of the vestibulocochlear nerve emerging from this capsule via the internal auditory foramen. CT images of vestibular organ were obtained in a 3D X-ray micro-CT system (Bruker microCT SkyScan 1172) with maximum resolution of 4.26 μ .

In addition, 3D reconstruction of labyrinth geometry was performed on the basis of MR-images of rats made in magnetic field of 11.7 T with resolution up to 30 μ (T2 mode) available in open access resource "Neuroimaging Informatics Tools and Resources Clearinghouse" (NITRC, <https://www.nitrc.org>). CT scanning and MRI reconstruction of the temporal bone resulted in a high-resolution visualization of 3D structure of the vestibular labyrinth with its location relatively to the reference anatomical coordinates. These data made it possible to exactly localize the puncture sites in temporal bone and precisely insert the electrodes.

During electrophysiological experiments, the specimens moistened with physiological saline were

fixed in a Petri dish placed under an MBS-10 stereoscope (Lytkarino Optical Glass Plant). The electrodes were inserted into the tissues of *bulla tympanica* and periotic capsule under visual control with the help of a micromanipulator (Laboratory Instruments Research and Development Establishment, Pushchino, Moscow Region, Russia). The stimulating electrode was inserted into the posterior semicircular canal of the vestibular organ and the recording electrode was attached to the nerve stump. The reference (common) electrode was placed in the tissues surrounding the *bulla tympanica* in the external and internal portions of acoustic meatus. The sinusoidal voltage pulses were delivered to the stimulating electrode from an SFG-2110 Function Generator (Good Will Instruments). Both stimulating voltage waveform and the transmitted voltage signal at the vestibular nerve were recorded with dual channel ASK-2034 oscilloscope (Aktakom). The constant electrical resistance of perilymph was measured with an 8845A Digit Precision Multimeter (Fluke) via the electrodes mounted in labyrinthine vestibule and in the cavity of posterior semicircular canal.

To simulate transmission of alternating electric current across the vestibular organ tissues, we developed a mathematical model with equivalent electric circuit of these tissues.

The data were analyzed statistically using R (Foundation of Statistical Computing) software. Normalcy of distribution was established with Shapiro—Wilk test. The results are summarized as $m \pm SD$.

RESULTS

A series of high-resolution CT images was obtained to examine anatomy and topography of rat vestibular labyrinth. The images allowed evaluation of the precise geometrical parameters of the osseous labyrinth of the rat vestibular apparatus (Table 1) and its location in the extracted osseous specimens (Fig. 1).

The resulting geometrical data made it possible to calculate the optimal perforation point for insertion of the stimulating electrode, which excluded lesion to the membranous labyrinth fraught with perilymph and endolymph mixing. The constructed anatomic 3D model of the inner ear was employed to determine the elec-

TABLE 1. Basic Sizes of Rat Vestibular Apparatus Elements Determined from High-Resolution CT Images (mm, $m \pm SE$)

Semicircular canals	Length	Midline diameter	Vestibule diameter	
			in the broadest portion	in the narrowest portion
Anterior	4.42 \pm 0.91	0.176 \pm 0.022	1.507 \pm 0.051	0.923 \pm 0.047
Posterior	4.29 \pm 0.22	0.186 \pm 0.022		
Lateral	4.49 \pm 0.13	0.183 \pm 0.031		

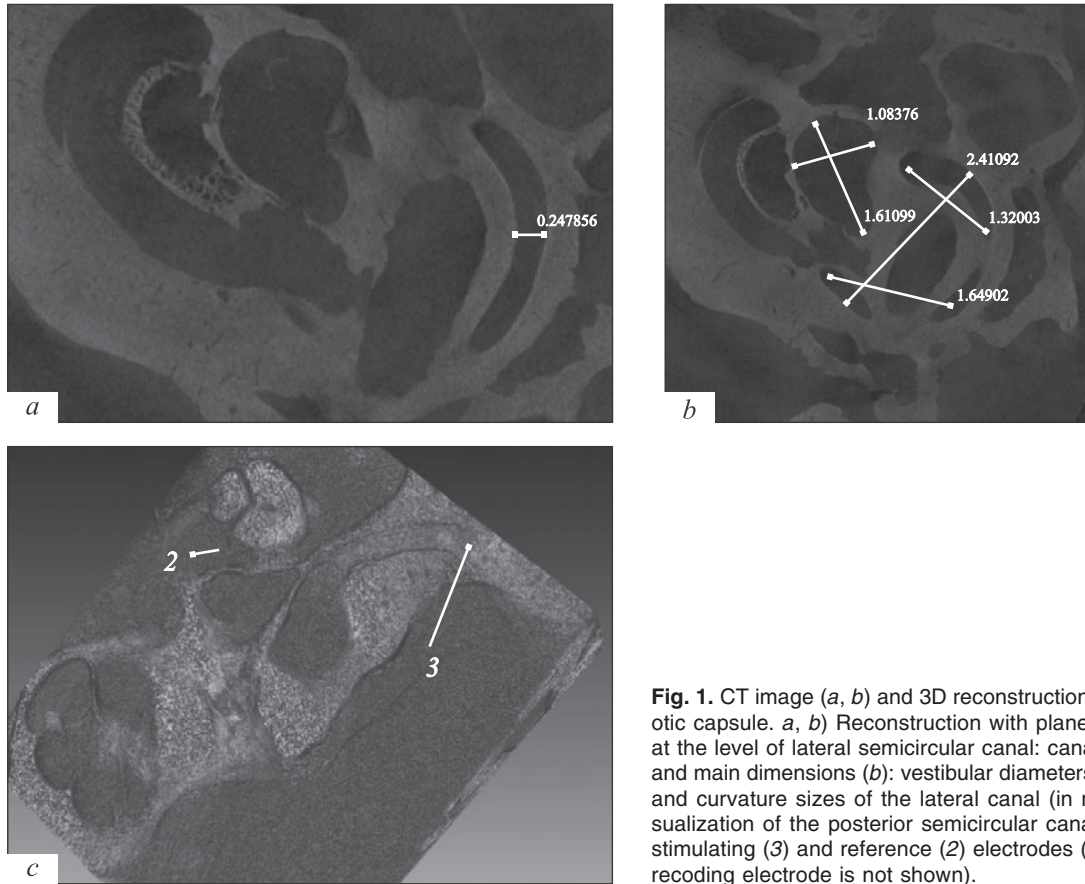


Fig. 1. CT image (*a, b*) and 3D reconstruction (*c*) of rat periotic capsule. *a, b* Reconstruction with plane cross-section at the level of lateral semicircular canal: canal diameter (*a*) and main dimensions (*b*): vestibular diameters and diameter and curvature sizes of the lateral canal (in mm). *c* 3D visualization of the posterior semicircular canal; locations of stimulating (*3*) and reference (*2*) electrodes (location of the recoding electrode is not shown).

trode layout relatively to the major anatomic structures at this ear portion. Thus, the stimulating electrode was inserted into the lumen of posterior semicircular canal and the recording electrode was placed on the vestibulo-cochlear nerve.

Then, we developed a mathematical model based on a premise that the biological tissues are electrically conducting media characterized with electrical impedance $Z=R+iX$. Its active component R describes mostly the electrical resistance of conducting internal electrolytic media. The reactive component $X=1/\omega C$ is determined by capacity of the stimulated tissue mostly reflecting the capacity of cell membranes [5,8]. The developed mathematical model of vestibular organ is based on its anatomic structure featuring the following elements: 1) the liquid medium with ionic conductivity and a certain specific resistance, 2) non-cellular structures characterized by specific resistance; and 3) cellular tissues described by membrane capacity and specific resistance of the intracellular liquid.

This model describes propagation of electric current across the vestibular labyrinth with due account for its anatomic structure, chemical composition of the biological fluids and tissues, and VI electrical parameters (Fig. 2) [2]. In the developed model, the electric current supplied through electrode implanted into

the perilymph space can spread in diverse directions across the tissues of vestibular labyrinth.

Actually, the electric current can propagate through the perilymph, which is a well-conducted electrolyte due to pronounced concentrations of organic and inorganic ions. In addition, the electrical signal can propagate decrementally across the labyrinthine membrane formed by epithelial and mesenchymal cells, travel further through endolymph to the ampullary cupula, cross it over, and finally excite the nerve terminals through the apical portion of neuroepithelium. Thus, the electrical impulse passing across *bulla tympanica* and periotic capsule will be loaded with electrical impedance, so its amplitude and phase will be transformed at the vestibular nerve input.

The character of these changes can be analyzed by employing the equivalent electrical models [3]. Here, the equivalent circuit is based on the rat vestibular apparatus geometry (Fig. 2). In this five-element Maxwell model, the electrical voltage pulse (I) generated at VI output and transmitted to stimulating electrode (I) travels to the recording electrode (2) across the tissues of vestibular labyrinth modelled with capacitors (C) and resistors (R). The gain—phase parameters of equivalent circuit were determined at the output (2) loaded with R_L resistance of 15 k Ω . All resistors and

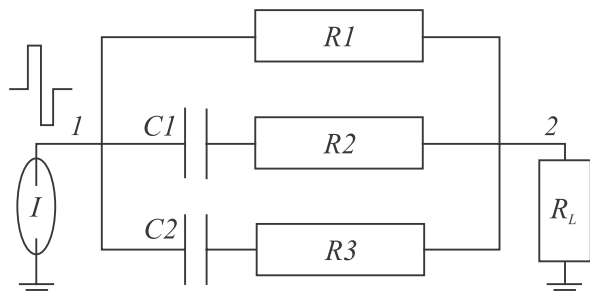


Fig. 2. Equivalent electrical scheme of vestibular labyrinth. *R1*: perilymph active resistance; *R_L*, load resistance. (*C1*, *R2*) and (*C2*, *R3*) are electrical parameters of the medium for the first and second variant of electrical current flow across the vestibular labyrinth tissues.

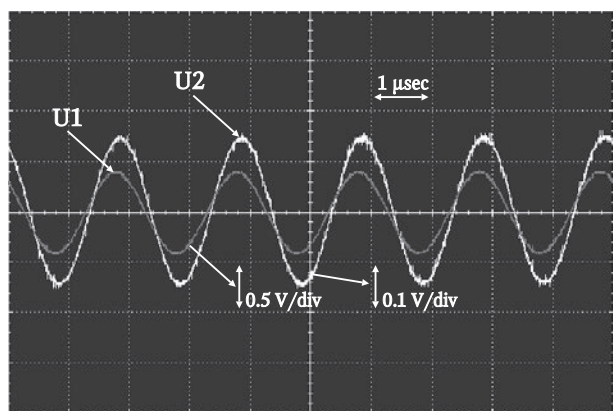


Fig. 3. Voltage oscillograms recorded from stimulating (*U1*) and recording (*U2*) electrodes at 500 Hz with reference electrode position (*1*) in acoustic meatus.

capacitors in the equivalent circuit were determined with due account for literature data (Table 2) and the results of anatomical reconstruction of the rat vestibular apparatus (Table 1, Fig. 1).

The electrophysiological measurements of the gain—phase characteristic of isolated vestibular preparation were carried out with the amplitude of stimulating waveform $U1=1$ V at frequency of 0.4-1.0 kHz. The reference electrode was positioned (*1*) in acoustic meatus of temporal bone near the oval window, (*2*) on the external surface of the temporal bone near acoustic meatus, and (*3*) on a segment of the temporal muscle.

The synchronous voltage signals in stimulating (*U1*) and recording (*U2*) electrodes were recorded in an oscilloscope (Fig. 3). The oscillograms showed the decrease of the amplitude of the output signal ($U2/U1 \gg 0.35$) and the time lag $t = \Delta\phi / (2\pi\nu) = 0.2$ μsec, where $\Delta\phi$ is the phase shift and ν is frequency of the signals. Virtually, the phase shift $\Delta\phi$ did not depend on the frequency within the specified frequency band. Both voltage attenuation and the phase shift were determined in relation to position of the reference electrode (Table 3).

The calculation of the phase shift in the equivalent mathematical model (Fig. 2) used the formula:

$$\text{tg}\Delta\phi = -\frac{[F(1-A\omega^2)-B\omega(1-D\omega^2)]}{BF\omega-(1-A\omega^2)(1-D\omega^2)}, [12]$$

where the constants *A*, *B*, *D*, and *F* were determined according to [2] with due account for vestibular labyrinth geometry and electrical parameters of vestibular apparatus (Tables 1, 2). In examined frequency range of 0.4-1.0 kHz, the time lag in the equivalent electrical circuit was 0.09 ± 0.06 μsec, which agrees with experimental data.

Thus, this study developed an *in vitro* electrophysiological model of electrical signal propagation through the tissues of vestibular apparatus and its equivalent mathematical representation based on CT and MRI anatomical data, which described the electrical impedance properties of the vestibular tissues. Both models yielded the measured and calculated gain—phase parameters of the electric current pathway from stimulating electrode to the vestibular nerve. They demonstrated the important role of reference electrode position in the vestibular apparatus. The developed electrophysiological and mathematical models can be used to optimize the transfer function of vestibular implants.

This work was supported by the Russian Science Foundation (grant No. 17-15-01249).

TABLE 2. Electrical Parameters of Tissues of the Vestibular Apparatus

Parameter	Value
Specific conductance	endolymph perilymph
	1.97 S/m 1.65 S/m
Electrical capacity of the hair cell membrane	30 pF
Electrical capacity of the membrane of cells forming the membranous labyrinth	23.8 pF
Electrical capacity of the membrane of the basal neuroepithelial cells	24.9 pF

TABLE 3. Gain—Phase Characteristic of Isolated Vestibular Preparation ($m \pm SE$)

Recorded signal/Reference electrode position	Acoustic meatus (position 1)	Temporal bone (position 2)	Temporal muscle (position 3)
Amplitude, V	0.15 ± 0.02	0.07 ± 0.02	0.08 ± 0.02
Phase shift, μsec	0.20 ± 0.05	0.10 ± 0.05	0.10 ± 0.05

REFERENCES

1. Voropayeva OF, Shokin YuI. Numerical simulation in medicine: formulations of the problems and some results of calculations. *Vychislit. Tekhnol.* 2012;17(4):29-55. Russian.
 2. Demkin VP, Shchetinin PP, Mel'nichuk SV, Kingma G, van de Berg R Pleshkov MO, Starkov DN. Propagation of electric current in tissues of human vestibular labyrinth: improvement of vestibular implant. *Izv. Vuzov. Fizika.* 2017;60(11):152-157. Russian.
 3. Zuev AL, Sudakov AI, Shakirov NV. Identical the electric model of biological objects. *Ross. Zh. Biomekh.* 2014;18(4):491-497. Russian.
 4. Kotova AB, Kiforenko SI, Belov VM. Mathematical modeling in biology and medicine. *Kibernetika Vychislit. Tekhnika.* 2013;(174):47-55. Russian.
 5. Nikolaev DV, Smirnov AV, Bobrinskaya IG, Rudnev SG. *Bioimpedance Analysis of Body Composition.* Moscow, 2009. Russian.
 6. Bradshaw AP, Curthoys IS, Todd MJ, Magnussen JS, Taubman DS, Aw ST, Halmagyi GM. A mathematical model of human semicircular canal geometry: a new basis for interpreting vestibular physiology. *J. Assoc. Res. Otolaryngol.* 2010;11(2):145-159.
 7. Gong W, Merfeld DM. Prototype neural semicircular canal prosthesis using patterned electrical stimulation. *Ann. Biomed. Eng.* 2000;28(5):572-581.
 8. Lionheart W, Polydorides N, Borsic A. The reconstruction problem. *Electrical Impedance Tomography: Methods, History and Applications.* Holder DS, ed. Manchester, 2004. P. 3-62.
 9. Lloret-Villas A, Varusai TM, Juty N, Laibe C, Le NovÈre N, Hermjakob H, Chelliah V. The impact of mathematical modeling in understanding the mechanisms underlying neurodegeneration: evolving dimensions and future directions. *CPT. Pharmacometrics Syst. Pharmacol.* 2017;6(2):73-86.
 10. Ramos Miguel A, Ramos Macías A, Viera Artiles J, Perez Zaballos MT. The Effect of Reference Electrode Position in Cochlear Implants. *J. Int. Adv. Otol.* 2015;11(3):222-228.
 11. Santos C.F, Belinha J, Gentil F, Parente M, Jorge RN. An alternative 3D numerical method to study the biomechanical behavior of the human inner ear semicircular canal. *Acta Bioeng. Biomech.* 2017;19(1):3-15.
 12. van de Berg R, Guinand N, Nguyen TA, Ranieri M, Cavuscens S, Guyot JP, Stokroos R, Kingma H, Perez-Fornos A. The vestibular implant: Frequency-dependency of the electrically evoked vestibulo-ocular reflex in humans. *Front. Syst. Neurosci.* 2015;8:255. doi: 10.3389/fnsys.2014.00255.
-